

# Development of Reactive Transport Models for Very High Temperature Heat Aquifer Storage (VESTA) at a Pilot Site in Germany

Ram Kumar<sup>1,2</sup>, Ghanashyam Neupane<sup>1,2</sup>, Wencheng Jin<sup>1</sup>, Trevor Atkinson<sup>1,2</sup>, Travis McLing<sup>1,2</sup>, Robert Smith<sup>2,3</sup>, Yingqi Zhang<sup>4</sup>, Patrick Dobson<sup>4</sup>, Eva Schill<sup>4,5</sup>, Thomas Kohl<sup>5</sup>, Florian Bauer<sup>5</sup>, Fabian Nitschke<sup>5</sup>, Judith Bremer<sup>5</sup>

<sup>1</sup>Idaho National Laboratory, Idaho Falls, Idaho, U.S.A., 83415

<sup>2</sup>Center for Advanced Energy Studies, Idaho Falls, Idaho, U.S.A., 83401

<sup>3</sup>Earth and Spatial Sciences, University of Idaho, Moscow, Idaho, U.S.A., 83844

<sup>4</sup>Lawrence Berkeley National Laboratory, Berkeley, California, U.S.A., 94720

<sup>5</sup>Karlsruhe Institute of Technology, Eggenstein-Leopoldshafen, Germany, 76344

## Keywords

*HT-RTES, Site Characterization, Geochemistry, Reactive Transport Processes, Thermal Short-circuiting, Scaling, Permeability Evolution*

## ABSTRACT

Thermal energy storage at large scale has significant potential for large scale clean energy deployment. However, it is necessary to understand and address the challenges (Dobson et al., 2023) associated with high temperature reservoir thermal energy storage (HT-RTES). Lessons learned from the previous demonstrations identify insufficient site characterization, thermal short-circuiting, lack of available heat, scaling, corrosion, and biofouling as key factors affecting the performance of HT-RTES. The objective of this paper is to develop reactive transport modeling strategies to understand the geochemical processes associated with HT-RTES in high-saline reservoirs by evaluating the significance of changes in temperature, pressure, mineralogy, and porosity of the formation during the HT-RTES operation. The results from the model will also evaluate the retrograde solubility of minerals, changes in permeability, and changes in redox conditions during the HT-RTES operation.

For this study, an isolated injection-production well doublet is used for injecting hot and cold fluids during the seasonal cycle. During summer, brine at 75 °C is surface heated to 140 °C and injected into the reservoir with 15% porosity. Produced brine from the heat-exchanger at 60 °C is injected back into the cold well during winter. Reactive transport simulations are carried out using TOUGHREACT-EOS7 (Dobson et al., 2004; Sonnenthal et al., 2021) for 5 years of cyclic RTES operation. Representative geochemical data were obtained from the depleted Leopoldshafen oil field of Leopoldshafen around the DeepStor site (Banks et al., 2021).

After a five-year operational period, the model estimates a 1.5% increase in the porosity in the vicinity of the hot wells. Near the cold wells, there is a negligible decrease in porosity, roughly

0.1%, within the same duration. These observations imply that dissolution of minerals is more prominent near the hot well because of the increase in temperature and the injection of slightly acidic brine, while mineral precipitation tends to occur near the cold well where the temperature falls. Iron minerals such as goethite show dissolution near the hot wells and precipitation in the relatively colder brine slightly away from the hot well. Also, changes in permeability have been evaluated using a cubic law of porosity-permeability correlation. There is no significant interference of hot and cold plumes, which indicates that thermal short-circuiting has not occurred under the simulated operating conditions. Future work will include a modeling scenario under strong oxidizing conditions such as presence of dissolved oxygen in the injection brine, which can better quantify the possibility of corrosion and scaling due to air intrusion.

## 1. Introduction

As the shift from fossil fuels to Variable Renewable Energy (VRE) technologies gains momentum for electricity generation and heating, the need for energy storage becomes more critical. While numerous energy storage systems are being developed to manage short-term needs, the significant seasonal fluctuations in VRE output and energy demand pose a greater challenge. Seasonal energy storage technologies, capable of transferring energy from periods of surplus such as summer to times of deficit like winter, are emerging as a vital solution. High-temperature reservoir thermal energy storage (HT-RTES) is being considered as a viable option for long-duration energy storage. This method allows the storage of surplus thermal energy in permeable geological formations like aquifers or depleted hydrocarbon fields over several months. While RTES demonstrates significant promise for geothermal energy applications at moderate temperatures (Fleuchaus et al., 2020), concerns about its long-term viability arise due to potential issues such as corrosion, scaling, and well clogging due to changes in geochemistry during the operation (Dobson et al., 2023) when shifting to higher temperatures.

This study aims to establish a method for assessing the impact of hydrogeochemical processes on RTES through the application of reactive transport modeling. The specific goals are 1) construct a numerical model for analyzing the reactive-transport processes relevant to RTES systems, 2) examine the geochemical factors which can impact system performance or diminished efficiency during cyclical operations, 3) determine the rates at which mineral precipitation and dissolution occur, and 4) assess alterations in porosity and permeability.

In terms of formation water chemistry, the DeepStor site at the Karlsruhe Institute of Technology (Germany) is used in this simulation. Notable research papers evaluating the potential of the DeepStor site for geothermal use include those by Banks et al. (2021), Frey et al. (2022), Bremer et al. (2022), Nitschke et al. (2023), Stober et al. (2023), Schill et al., (2024), and Stricker et al. (2024). Banks et al. (2021) conducted a preliminary geochemical evaluation, identifying potential risks such as mineral scaling and structural damage in the reservoir due to reactive transport processes, with a particular emphasis on reduced porosity around the thermal wells. The study utilized a model based on equilibrium thermodynamics to simulate the dissolution and precipitation of minerals. However, equilibrium thermodynamics may not yield precise predictions for the rates of mineral dissolution and precipitation. To enhance the accuracy of modeling results, it is important to incorporate reaction kinetics. Nitschke et al. (2023) conducted an analysis of brine-rock interactions and scaling potential, employing the MulT\_predict geothermometer to analyze the chemical system's temperature control. The study identified key scaling minerals such as iron hydroxides, calcite, celestite, and barite, noting distinct scaling mechanisms during both

the testing phase with open pond storage and the operational phase with a two-well system for cyclic storage and production. However, the study did not integrate transport processes, which could impact the geochemical processes related to brine-rock interaction during cyclic RTES operations.

This study aims to bridge current knowledge gaps by evaluating the DeepStor site for RTES through a reactive-transport modeling approach.

## 2. Methodology

### 2.1 Geologic and Hydraulic Setting at DeepStor site

The DeepStor site is situated at KIT Campus North, nestled within the central portion of the Upper Rhine Graben (URG), a key segment of the European Cenozoic Rift System. This region is known for Germany's most significant temperature anomaly, reaching approximately 170°C at 3,000 meters depth (Baillieux et al., 2013). Over 2,000 meters of sediment have accumulated at the DeepStor location, predominantly under shallow marine conditions, leading to substantial marl deposits interspersed with layers of sand. The targeted strata for DeepStor, the calcareous fine-grained sandstones of the Niederrödern and Froidefontaine Formations, are found at depths of approximately 800 and 1,300 meters, respectively (Bremer et al., 2022). These sandstone layers reach thicknesses of up to 10 meters and exhibit subsurface temperatures between 70-90°C. The hydrologic and thermal characteristics of the sandstones in the Meletta beds from the Froidefontaine Formations have been described by Banks et al. (2021) and Stricker et al. (2024). These properties have been employed while setting up simulations in the current study. To generalize the approach, the site-specific and rather limited thickness of the sandstone layer of the Niederrödern and Froidefontaine Formations has been increased to a thickness of 220 m. In the first approach, the vertical temperature gradient has been neglected. Also, precipitation of minerals during the surface heating and cooling processes are not considered in this study.

**Table 1: Hydrologic and thermal properties of the units used in modeling, adapted from Banks et al. (2021) and Stricker et al. (2024).**

Unit	Porosity	Permeability (m <sup>2</sup> )	Thermal Conductivity (Wm <sup>-1</sup> K <sup>-1</sup> )	Grain Heat Capacity (J/kg/°C)	Grain Density (kg/m <sup>3</sup> )
Sandstone	0.15	6.6×10 <sup>-14</sup>	2.50	850	2680
Caprock	0.01	2.1×10 <sup>-18</sup>	1.50	964	2630

### 2.2. Numerical modeling approach

Reactive transport modeling was performed using TOUGHREACT V4 (Sonnenthal et al., 2021). The Equation of State module (EOS7) used for the modeling considers aqueous phases not as mixtures of water and salt but as mixtures of water and brine. The salinity of the aqueous phase is described by means of the brine mass fraction, and density and viscosity are interpolated from the values for the water and brine endmembers. The brine is modeled as NaCl solution. The model does not account for changes in enthalpy due to salinity. Fluid flow within this system are governed

by Darcy's law, as described by Pruess et al. (1999), while heat transfer is facilitated by both conduction and convection, incorporating both sensible and latent heat changes.

In the liquid phase, aqueous species are transported and interact with the solid and gas phases. The chemical transport equations use total dissolved concentrations, including primary species and their secondary aqueous counterparts (Sonnenthal et al., 2021). The kinetics of mineral dissolution and precipitation are based on the Transition State Theory, following the work of Steefel and Lasaga (1994) and Xu and Pruess (2001), expressed as follows:

$$r_n = \pm A_n k_n (1 - \Omega_n^\theta)^\eta \quad n = 1 \dots N_q \quad (1)$$

where  $k_n$  is the rate constant (moles/mineral surface area/time),  $A_n$  is the specific reactive surface area/kg of  $H_2O$ ,  $\Omega_n$  is the ratio of the activity product (Q) divided by the equilibrium constant (K). A positive value of  $r_n$  indicates mineral dissolution and a negative value indicates mineral precipitation.

Permeability changes are calculated from porosity change using ratios of permeabilities calculated from the Carman-Kozeny relation (Bear, 1972) as follows:

$$k = k_i \frac{(1-\phi_i)^2}{(1-\phi)^2} \left( \frac{\phi}{\phi_i} \right)^3 \quad (2)$$

$\phi_i$  and  $k_i$  denotes initial porosity and initial permeability respectively.

### 2.3. Griding and RTES parameters

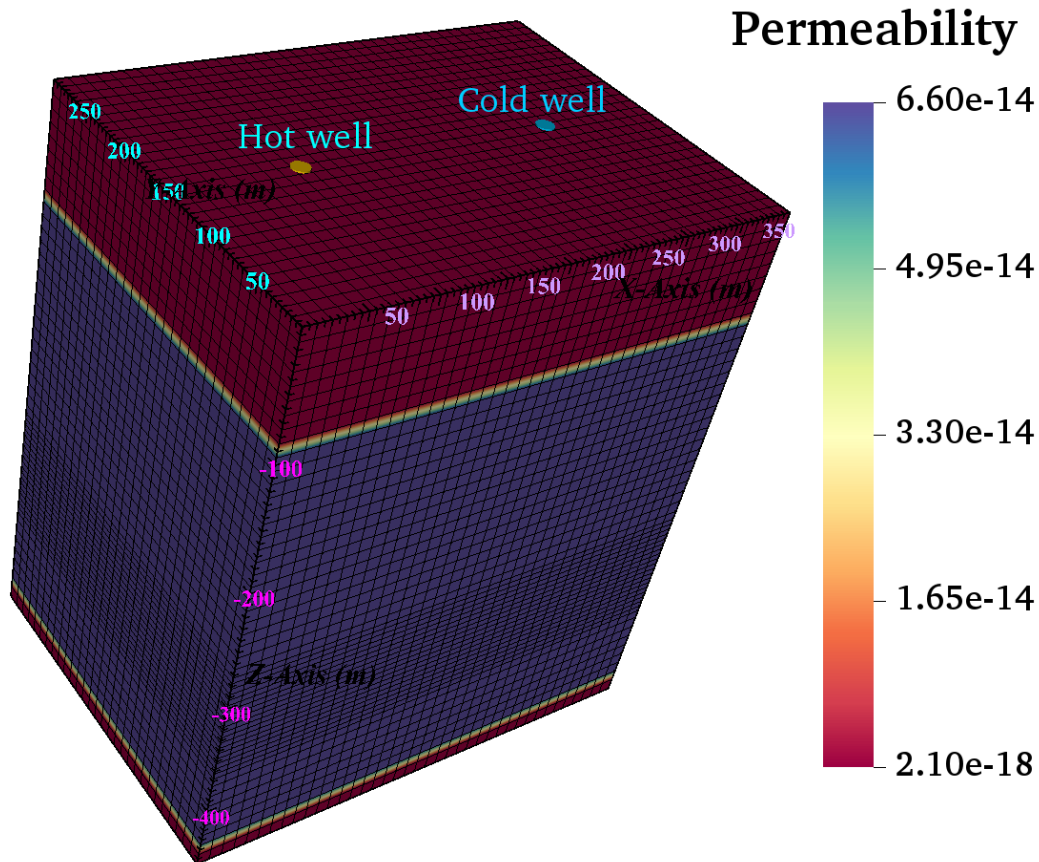


Figure 1: 3-D gridding of the mesh with initial permeability.

A finely discretized three-dimensional grid has been developed, tailored to the characteristics of the storage rock formations. The initial permeability for both the Niederrödern and Froidefontaine Formations has been uniformly set across the grid, with increased resolution near the injection zones as shown in Figure 1. The constructed mesh omits the overlaying strata up to a depth of 1000 meters, focusing exclusively on the Niederrödern and Froidefontaine Formations to optimize computational efficiency. The grid incorporates site-specific vertical pressure gradients to establish initial pressure conditions, maintaining a constant temperature profile. At the base level of the grid ( $Z=0$  meters) represents the pressure conditions found at 1 kilometer depth at the actual site location. To avoid the thermal short-circuiting during injection and extraction processes, hot and cold wells are positioned 200 meters apart (Figure 1), each with a 50-meter screen segment, operating at a flow rate of 5 kg/s. In first run a steady state simulation is performed to obtain hydrostatic pressure conditions, and the results from this run is used as boundary condition in second run to simulate undisturbed natural state conditions with throughflow of mass and heat. In third run, the operational cycle begins with the injection of hot brine at 140°C into the hot well for six months during the summer, while the cold well simultaneously produces at the same rate. For the following six months, brine at 60°C is injected into the cold well, with the hot well producing at an equivalent rate. The study simulates this cyclic procedure over a period of five years.

### ***2.3. Mineralogy and brine chemistry***

For the reactive transport simulations, the mineral compositions and proportions are informed by Banks et al. (2021) and comprise primary minerals such as quartz, calcite, dolomite, albite, muscovite, microcline, annite, clinocllore, and kaolinite. Additionally, secondary minerals such as goethite, hematite, and ferrihydrite have been incorporated into the model. The mineral kinetic rate parameters are adapted from Palandri and Kharaka (2004).

The brine chemistry or fluid composition (Table 2) at Meletta Beds of Froidefontaine Formation in the Leopoldshafen field is reported by on Banks et al. (2021).  $Al^{3+}$  is calculated by assuming equilibrium with albite. The brine is further speciated for near steady state concentrations with minerals at 75°C using the thermodynamic database from Blanc et al. (2007). The steady-state brine chemistry is also speciated at 60°C and 140°C to align the temperatures of injection fluids in cold and hot wells respectively.

First scope calculations have been conducted accounting for a DeepStor type system consisting of a doublet with a warm and a cold leg. The calculations adopt the DeepStor strategy assuming the wells to be separated not to exchange thermal energies in the underground. These conceptual models intend to demonstrate the possible influence of hydrochemistry on thermal storage systems.

**Table 2: Brine speciation calculated to mimic near steady-state brine composition with minerals at 75°C and 140°C. Al<sup>3+</sup> is estimated by equilibrating the solution with albite using Blanc et al. (2012).**

Primary Species	Speciated concentration at 75°C (molal)	Speciated concentration at 140°C (molal)
pH	7.24	6.53
Ca <sup>2+</sup>	9.250×10 <sup>-02</sup>	9.249×10 <sup>-02</sup>
Fe <sup>2+</sup>	1.207×10 <sup>-05</sup>	1.207×10 <sup>-05</sup>
Mg <sup>2+</sup>	3.348×10 <sup>-02</sup>	3.349×10 <sup>-02</sup>
Na <sup>+</sup>	1.647×10 <sup>-00</sup>	1.647×10 <sup>-00</sup>
K <sup>+</sup>	1.557×10 <sup>-02</sup>	1.557×10 <sup>-02</sup>
Cl <sup>-</sup>	1.907×10 <sup>-00</sup>	1.908×10 <sup>-00</sup>
HCO <sub>3</sub> <sup>-</sup>	2.310×10 <sup>-04</sup>	2.311×10 <sup>-04</sup>
SO <sub>4</sub> <sup>2-</sup>	5.166×10 <sup>-03</sup>	5.166×10 <sup>-03</sup>
Al <sup>3+</sup>	1.734×10 <sup>-8</sup>	1.738×10 <sup>-8</sup>
SiO <sub>2</sub> (aq)	5.822×10 <sup>-04</sup>	5.823×10 <sup>-04</sup>
O <sub>2</sub> (aq)	3.153×10 <sup>-63</sup>	3.154×10 <sup>-63</sup>

### 3. Results and discussion

#### 3.1. Evolution of temperature during seasonal operation

Figure 2 illustrates the temperature variations in the hot and cold wells after 5 years of seasonal operations. The spatial distribution of thermal energy across the XZ-plane at Y=145 m is depicted, highlighting the thermal dynamics around the wells. The cold well is injected with brine at 60°C, resulting in a cooler region surrounding them. Conversely, the hot well receives heated brine at 140°C, which then propagates outward, eventually encountering and mixing with the native colder brine, creating a cooler thermal front further from the well.

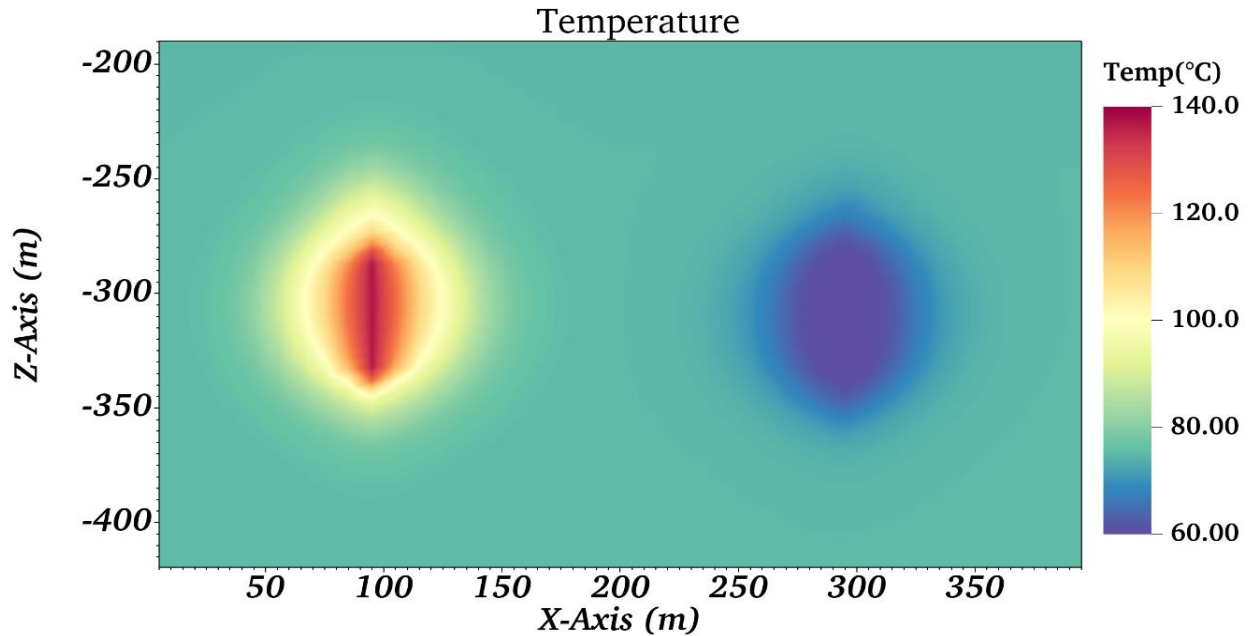


Figure 2: Variation of temperature at a hot and a cold well after 5 years of seasonal injection and production cycles.

### 3.2. pH and concentrations of iron species

Variations in pH and the concentrations of iron species ( $\text{Fe}^{2+}$  and  $\text{Fe}^{3+}$ ) serve as significant indicators of the extent to which brine chemistry can influence mineral dissolution and precipitation, as well as the redox potential for iron oxidation, which are critical factors in the formation of scale and the occurrence of corrosion. In Figure 3, the pH levels around the hot and cold wells are depicted, indicating an increase in pH to about 7.5 near the cold well and a decrease to approximately 6.4 around the hot well. These pH shifts can be ascribed to the water-rock interactions and the temperature-dependent changes in the activity coefficient of  $\text{H}^+$  associated with change in dissociation constant of water.

Figures 4 and 5 show the concentrations of ferrous ( $\text{Fe}^{2+}$ ) and ferric ( $\text{Fe}^{3+}$ ) ions respectively, with a notable increase in iron species concentrations around the hot wells relative to the cold wells. Plotting individual ferrous and ferric ion concentrations instead of total concentrations provides insight into the oxidizing or reducing conditions that may result in the precipitation of iron-containing minerals. This situation could pose a risk of corrosion to the well bore and tubing. The marked contrast between the concentrations of  $\text{Fe}^{2+}$  and  $\text{Fe}^{3+}$  suggests that the current model does not incorporate the effects of oxygen intrusion or potent oxidizing conditions. In oxidizing environments, there would likely be a greater conversion of  $\text{Fe}^{2+}$  to  $\text{Fe}^{3+}$ , which in turn could amplify the risk of precipitation of Fe (III) minerals such as goethite. At this point, the study doesn't consider intrusion of oxygen at the surface.

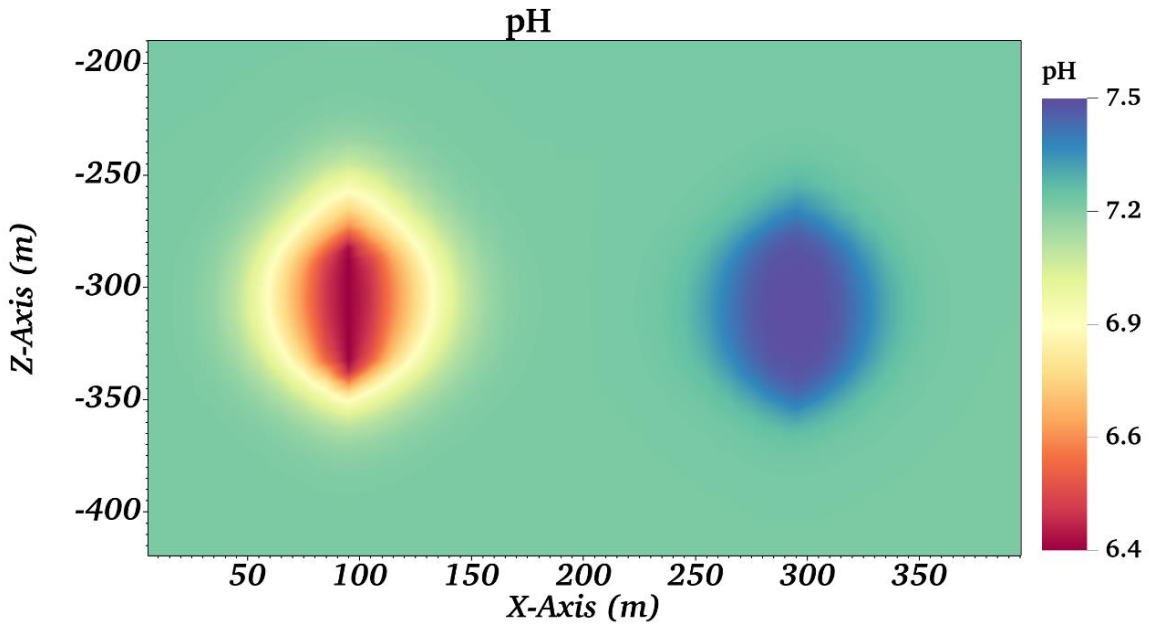


Figure 3: pH distribution in the XZ-plane (Y=145 m) after 5 years of seasonal injection and production cycles.

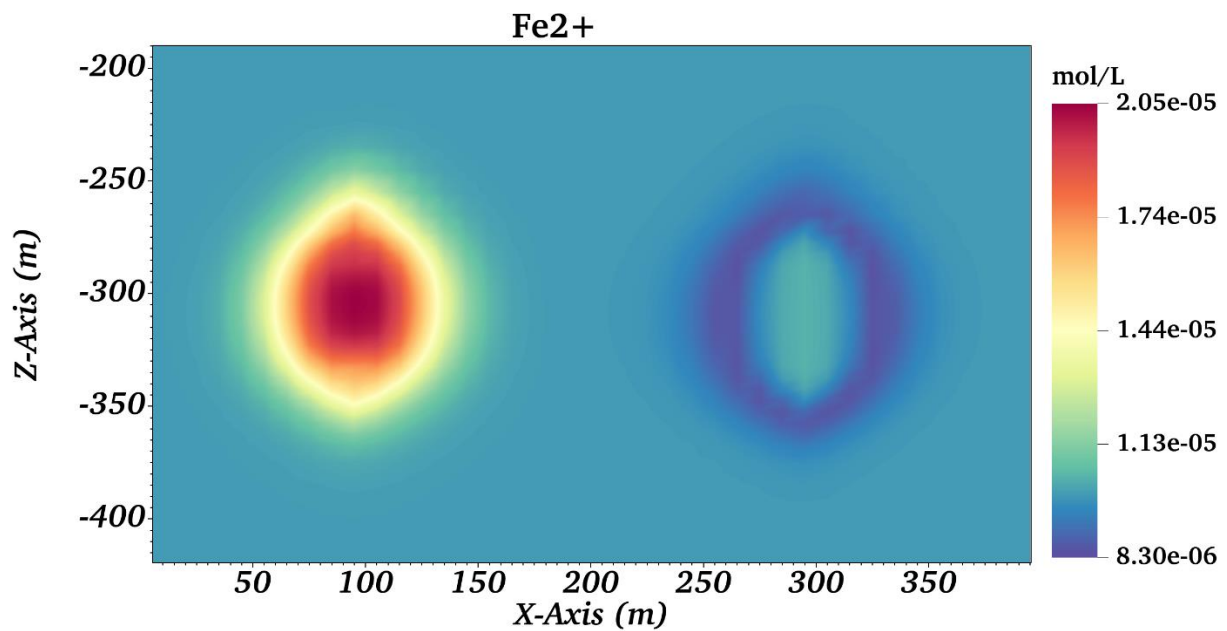


Figure 4: Concentration (mol/L) of  $\text{Fe}^{2+}$  in the XZ-plane (Y=145 m) after 5 years of seasonal injection and production cycles.

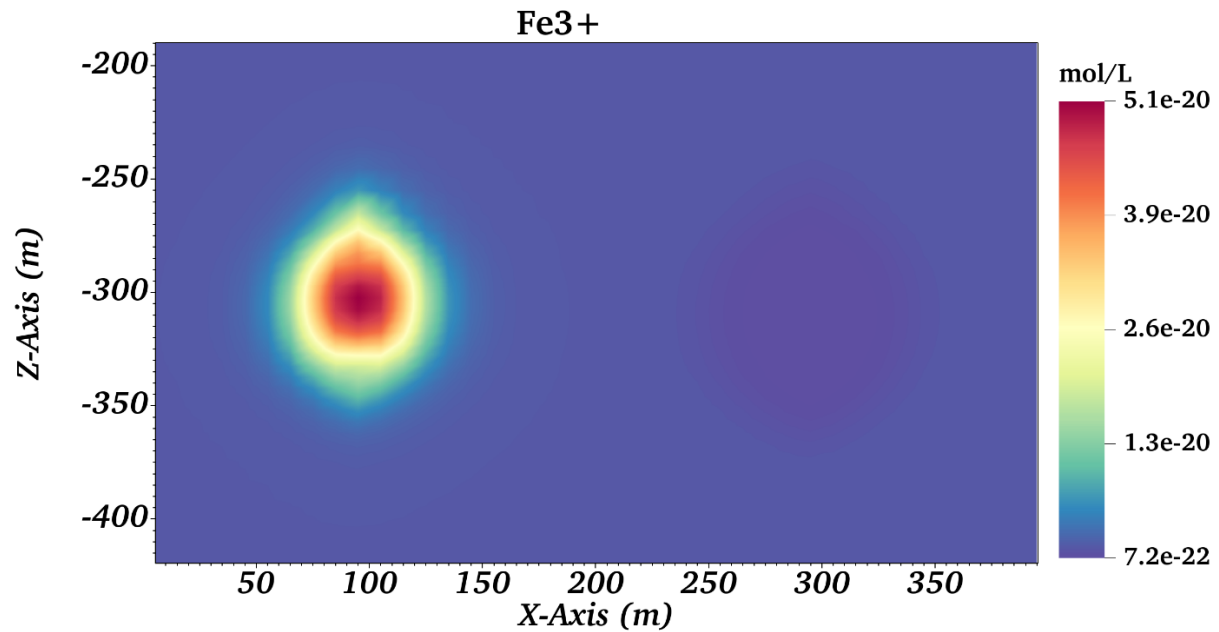


Figure 5: Concentration (mol/L) of  $\text{Fe}^{3+}$  in the XZ-plane ( $Y=145$  m) after 5 years of seasonal injection and production cycles.

### 3.3. Changes in mineralogy

#### 3.3.1. Changes in calcite and dolomite

Changes in calcite and dolomite in terms of volume fraction of total minerals are plotted in Figure 6 and 7, respectively. The model forecasts the dissolution of calcite near the hot well, likely due to the mildly acidic characteristics of the injected brine when subjected to elevated temperatures. However, the formation of dolomite is predicted in the areas adjacent to the hot well. Near the cold well, the situation reverses with calcite forming and dolomite dissolving. It is important to note that the mineralogical alterations of calcite and dolomite near the cold well are approximately an order of magnitude less compared to those near the hot well.

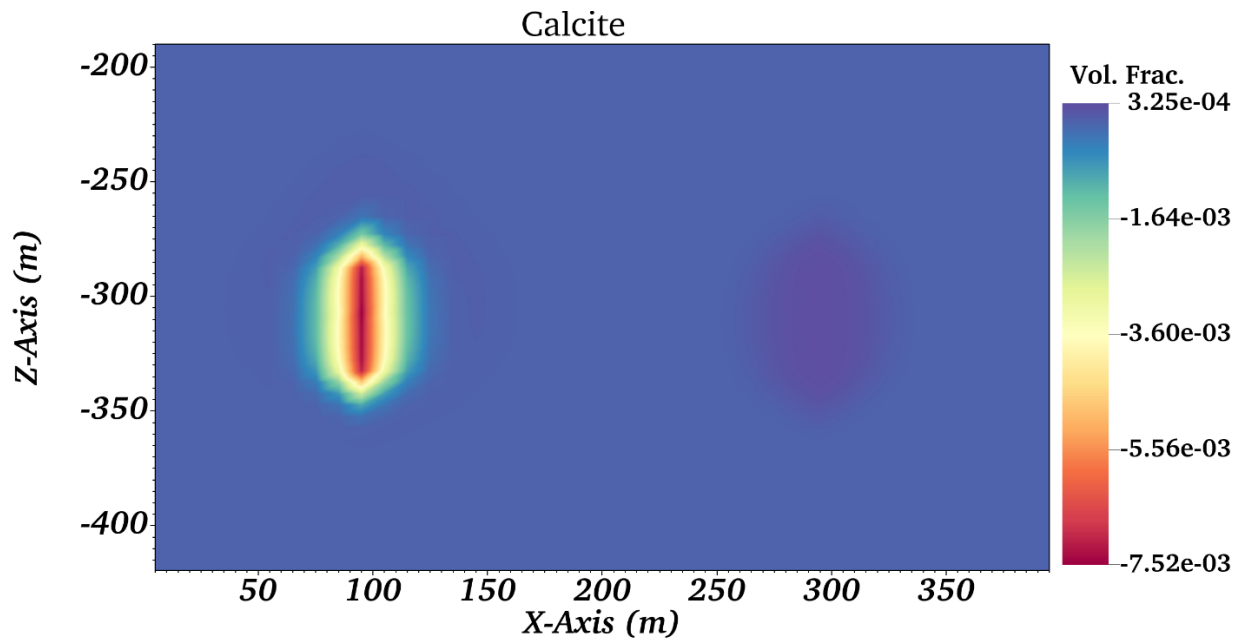


Figure 6: Calcite changes (volume fraction) in the XZ-plane (Y=145 m) after 5 years. A negative value on color bar indicates dissolution whereas a positive value indicates precipitation.

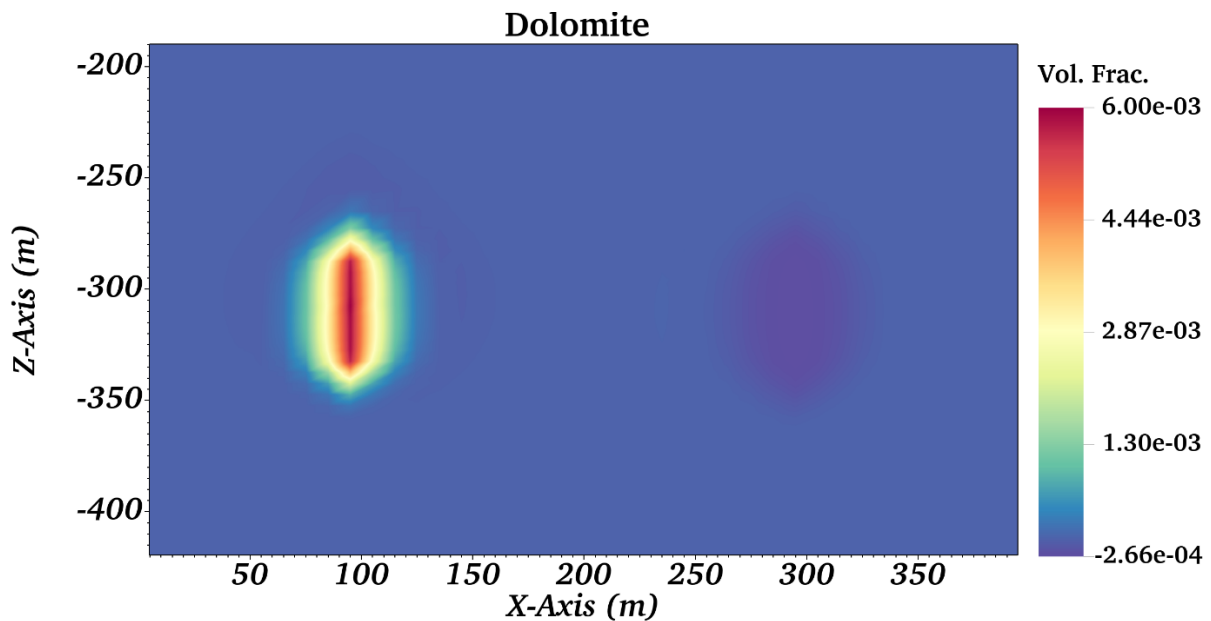
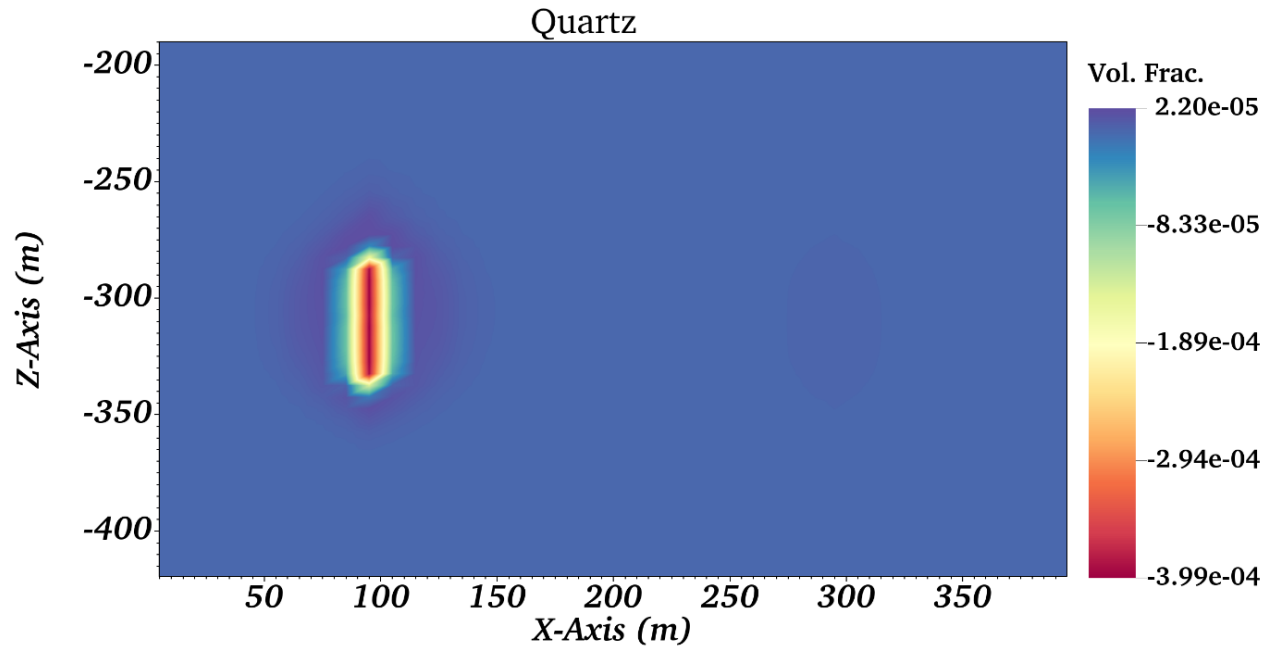


Figure 7: Dolomite changes (volume fraction) in the XZ-plane (Y=145 m) after 5 years of seasonal injection and production cycles.

### 3.3.2. Changes in quartz and microcline

Figures 8 and 9 illustrate that quartz and microcline undergo dissolution in proximity to the hot well, while precipitation of these minerals near the cold wells is observed to be substantially lower, with the rate of precipitation being about 20 and 50 times smaller in magnitude relative to the dissolution rates.



**Figure 8:** Changes in quartz (volume fraction) in the XZ-plane (Y=145 m) after 5 years of seasonal injection and production cycles.

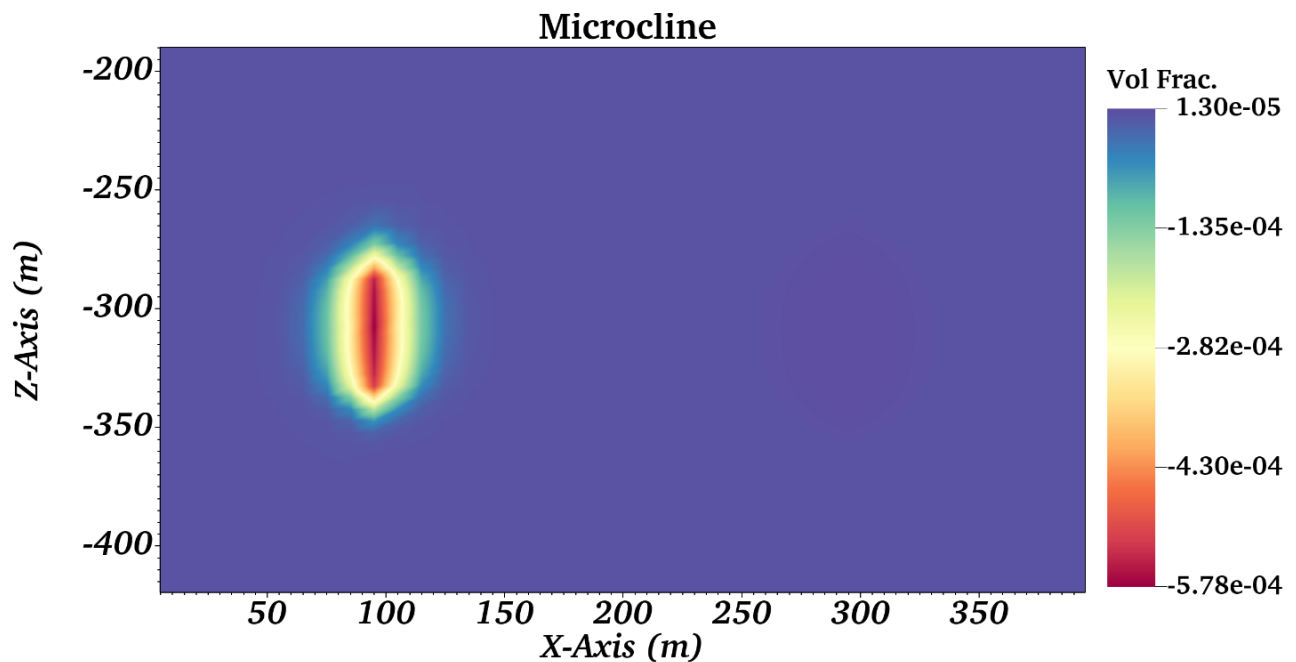


**Figure 9:** Changes in microcline (volume fraction) in the XZ-plane (Y=145 m) after 5 years of seasonal injection and production cycles.

### 3.3.3. Changes in goethite and hematite

In Figure 10, it is observed that goethite dissolves near the wellbore where the temperature is around 140°C. However, at a distance from the wellbore where the temperature drops, goethite precipitation occurs, matching the scale of dissolution seen in the warmer region. The precipitation

of hematite (Figure 11) near the hot well is observed to be roughly 15 times less in magnitude compared to the changes in goethite. Neither of the iron minerals, hematite and goethite, exhibit significant changes in the vicinity of the cold wells.

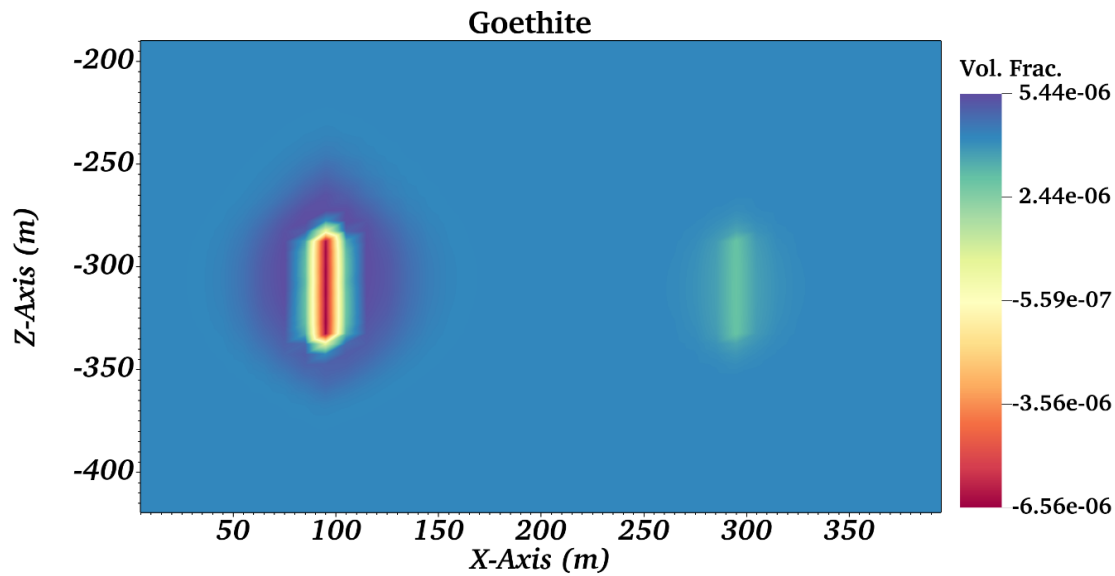


Figure 10: Changes in goethite (volume fraction) in the XZ-plane ( $Y=145$  m) after 5 years of seasonal injection and production cycles.

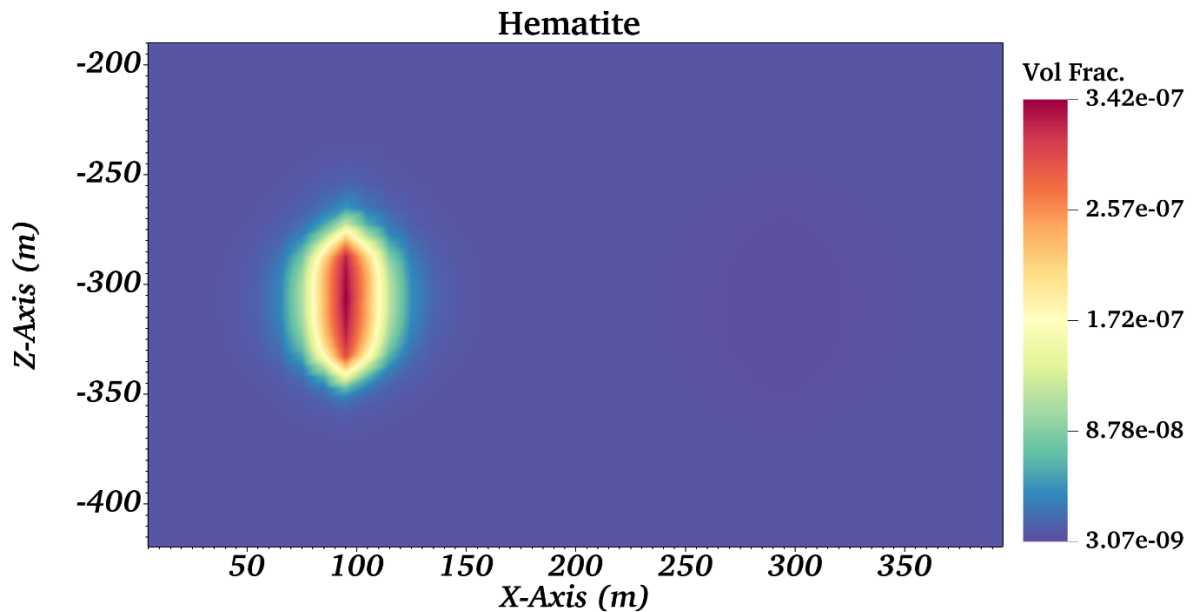


Figure 11: Changes in hematite (volume fraction) in the XZ-plane ( $Y=145$  m) after 5 years of seasonal injection and production cycles.

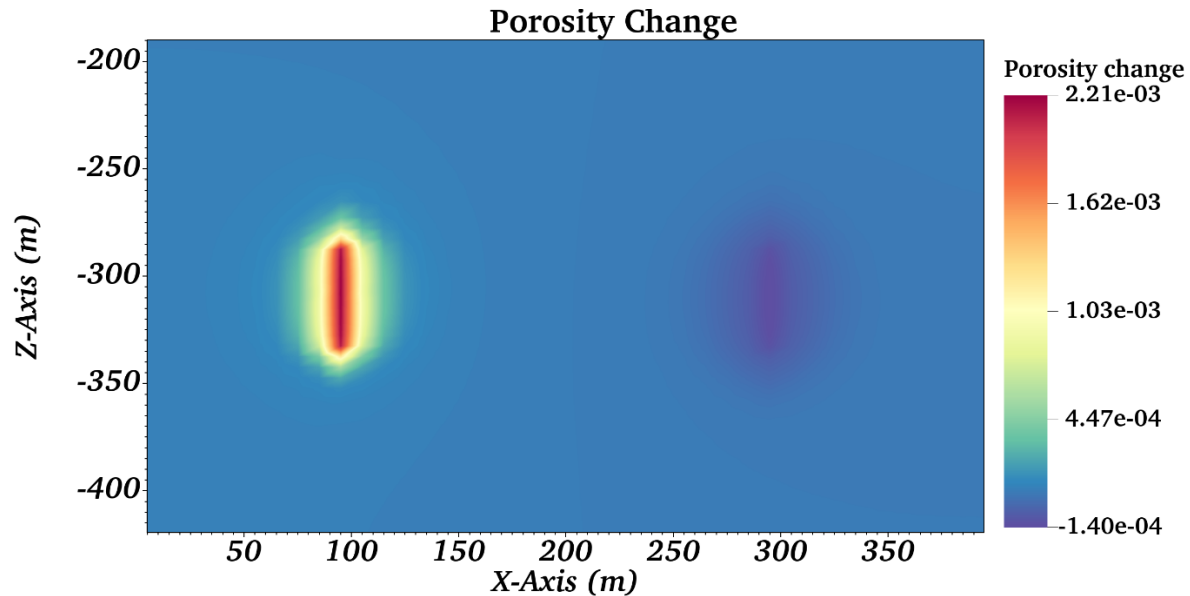


Figure 12: Changes in porosity in the XZ-plane (Y=145 m) after 5 years of seasonal injection and production cycles.

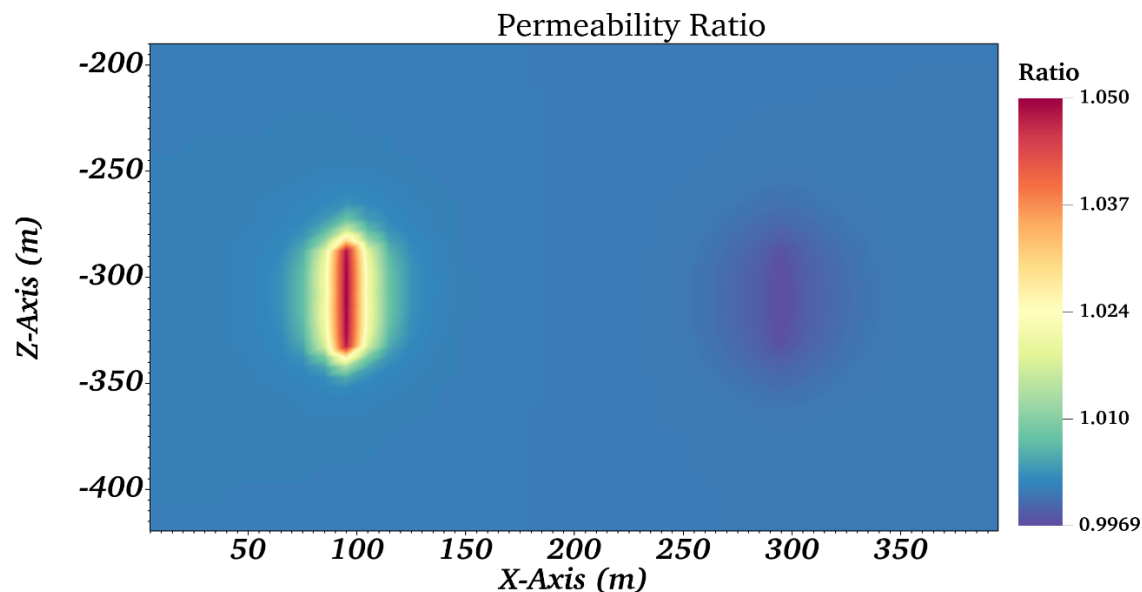


Figure 13: Permeability ratio in the XZ-plane (Y=145 m) after 5 years of seasonal injection and production cycles.

### 3.4. Changes in porosity and permeability

Figure 12 illustrates the overall variations in porosity attributed to the dissolution and precipitation of minerals. The modeling indicates an increase in porosity of around 1.5% in the area surrounding the hot well, while a decrease of approximately 0.1% in porosity is predicted near the cold well. The enhanced porosity observed near the hot well can be linked to the dissolution of calcite, quartz, and microcline, with calcite undergoing the most significant amount of dissolution among these minerals. The amount of dolomite that precipitates near the hot well is not as substantial as the

combined dissolution of these minerals, which leads to a net increase in porosity. This augmented porosity adjacent to the hot well may improve the efficacy of the injection process for long-term storage, and the minimal decrease in porosity near the cold well is considered to have little impact. Figure 13 depicts the permeability ratio, which is calculated as the current permeability divided by the initial permeability. This ratio is derived from changes in porosity, using a cubic law for the calculation.

#### 4. Conclusions and future work

The conceptual model integrates operational conditions, hydrogeologic attributes, and mineralogical data to simulate outcomes such as heat distribution, the likelihood of thermal short-circuiting, and variations in pH, brine composition, mineralogy, porosity, and permeability. The conclusions drawn from this study reveal that, over a five-year period, the operation of the RTES system within the established operational and reservoir parameters carries no significant risk. Results from the reactive transport modeling can guide the optimization of operational practices to enhance the effectiveness of thermal energy storage and reduce the incidence of operational failures owing to corrosion and scaling, which stem from retrograde solubility and the precipitation of iron minerals. Additionally, the findings from this study can be utilized to develop preventative measures to circumvent these issues, thereby promoting the sustainability of long-term reservoir thermal energy storage.

Future directions for this research will account for a refined geometrical setting and will include modeling scenarios with strong oxidizing conditions, like the presence of dissolved oxygen, to better quantify the potential for corrosion and scaling resulting from air intrusion. Also, it will be necessary to refine the grid resolution around the well to millimeter-scale accuracy to more precisely quantify the precipitation of iron hydroxides on the well screen. Also, a detailed wellbore simulation can be integrated with the reservoir simulation to better quantify the mineralogical changes at well screens.

#### Acknowledgement

We express our gratitude to the United States Department of Energy (DOE) and the German Federal Ministry of Education and Research (BMBF) for their financial contribution to our research as part of the VESTA project. We also acknowledge the support from Neptune Energy GmbH and their consortium partners. The research is funded by the U.S. Department of Energy's Office of Energy Efficiency and Renewable Energy, Geothermal Technologies Office, with Lawrence Berkeley National Laboratory being funded under Award Number DE-AC02-05CH11231 and Idaho National Laboratory under Award Number DE-AC07-05ID14517.

#### REFERENCES

- Baillieux, P., Schill, E., Edel, J.-B., and Mauri, G. "Localization of temperature anomalies in the Upper Rhine Graben: insights from geophysics and neotectonic activity". *International Geology Review*, v. 55, no. 14, (2013), p. 1744-1762.
- Banks, J., Poulette, S., Grimmer, J., Bauer, F., and Schill, E. "Geochemical Changes Associated with High-Temperature Heat Storage at Intermediate Depth: Thermodynamic Equilibrium

- Models for the DeepStor Site in the Upper Rhine Graben, Germany". *Energies*, v. 14, no. 19, (2021), p. 6089.
- Bear, J., 1972, "Dynamics of Fluid in Porous Media", New York, Dover Publications, Inc.
- Blanc, P., Lassin, A., Piantone, P., Azaroual, M., Jacquemet, N., Fabbri, A., and Gaucher, E. C. "Thermoddem: A geochemical database focused on low temperature water/rock interactions and waste materials". *Applied Geochemistry*, v. 27, no. 10, (2012), p. 2107-2116.
- Blanc, P., Lassin, A., Piantone, P., and Burnol, A. "Thermoddem a database devoted to waste minerals". *Bureau de Recherches Géologiques et Minières (Orléans, France)*, (2007), p.
- Bremer, J., Nitschke, F., Bauer, F., Schill, E., Kohl, T. Kaymacki, E., Koelbel, T., El-Alfy, A., Ollinger, D., Meier, P., Pei, L., Blöcher, G., Klein, S., Hahn, F., Atkinson, T.A., McLing, T., Jin, W., Zhang, Y., Dobson, P., Rutqvist, J., Hörbrand, T., and Jahrfeld, T. "VESTA – Very-high-temperature heat aquifer storage". European Geothermal Congress 2022, Berlin, Germany, (2022), 5 p.
- Dobson, P. F., Atkinson, T. A., Jin, W., Acharya, M., Akindipe, D., Li, B., McLing, T., and Kumar, R., Hybrid Uses of High-Temperature Reservoir Thermal Energy Storage: Lessons Learned from Previous Projects, SPE Energy Transition Symposium, 2023, p. D011S001R001.
- Dobson, P. F., Salah, S., Spycher, N., and Sonnenthal, E. L. "Simulation of water–rock interaction in the Yellowstone geothermal system using TOUGHREACT". *Geothermics*, v. 33, no. 4, (2004), p. 493-502.
- Fleuchaus, P., Schüppler, S., Godschalk, B., Bakema, G., and Blum, P. "Performance analysis of Aquifer Thermal Energy Storage (ATES)". *Renewable Energy*, v. 146, (2020), p. 1536-1548.
- Frey, M., Bär, K., Stober, I., Reinecker, J., van der Vaart, J., and Sass, I. "Assessment of deep geothermal research and development in the Upper Rhine Graben". *Geothermal Energy*, v. 10, no. 1, (2022), p. 18.
- Nitschke, F., Ystroem, L., Bauer, F., and Kohl, T. Published, "Geochemical constraints on the operations of high temperature aquifer energy storage (HT-ATES) in abandoned oil reservoirs", in *Proceedings Proceedings, 48th Workshop on Geothermal Reservoir Engineering, Stanford University, Stanford, California (2023)*.
- Palandri, J. L., and Kharaka, Y. K. "A compilation of rate parameters of water-mineral interaction kinetics for application to geochemical modeling". U.S. Geological Survey Open File Report 2004-1068, 2004.
- Pruess, K., Oldenburg, C. M., and Moridis, G. "TOUGH2 user's guide version 2". Lawrence Berkeley National Lab.(LBNL), Berkeley, CA (United States), 1999.
- Schill, E., Knauth, R., Garipi, X., and Bauer, F. DeepStor - Heat cycling in the deep and medium-deep subsurface. Proceedings, 49<sup>th</sup> Workshop on Geothermal Reservoir Engineering, Stanford University, Stanford, CA, (2024).
- Sonnenthal, E., Spycher, N., Xu, T., and Zheng, L. "TOUGHREACT V4.1-OMP reference manual: a parallel simulation program for non-isothermal multiphase geochemical reactive transport". University of California, Berkeley., (2021).
- Steeffel, C. I., and Lasaga, A. C. "A coupled model for transport of multiple chemical species and kinetic precipitation/dissolution reactions with application to reactive flow in single phase hydrothermal systems". *American Journal of Science*, v. 294, (1994), p. 529-592.

- Stober, I., Jäggle, M., and Kohl, T. "Optimizing scenarios of a deep geothermal aquifer storage in the southern Upper Rhine Graben". *Geothermal Energy*, v. 11, no. 1, (2023), p. 34.
- Stricker, K., Egert, R., Schill, E., and Kohl, T. "Risk of surface movements and reservoir deformation for high-temperature aquifer thermal energy storage (HT-ATES)". *Geothermal Energy*, v. 12, no. 1, (2024), p. 4.
- Xu, T., and Pruess, K. "On fluid flow and mineral alteration in fractured caprock of magmatic hydrothermal systems". *Journal of Geophysical Research: Solid Earth*, v. 106, no. B2, (2001), p. 2121-2138.